

## CFD ANALYSIS FOR UAV OF FLYING WING

**Dumitru PEPELEA, Marius Gabriel COJOCARU, Adrian TOADER, Mihai Leonida NICULESCU**

National Aerospace Research, București, Romania  
 (pepelea.dumitru@incas.ro, cojocaru.gabriel@incas.ro, toader.adrian@incas.ro,  
[niculescu.mihai@incas.ro](mailto:niculescu.mihai@incas.ro))

DOI: 10.19062/2247-3173.2016.18.1.22

**Abstract:** *The range of unmanned aerial aircraft (UAV) is developing continuously generating new constructive solutions from small size and mass to those, which are comparable to piloted aircraft. The main reason of UAV use is due to lower cost of design, realization and operation (on flight hour) in comparison with human piloted aircraft. This paper presents the CFD analysis on a UAV tailless, after a 3D scanned real model.*

**Keywords:** *CFD, UAV, flying wing, aerodynamic parameters*

### *Symbols and acronyms*

$\rho$	<i>Air density</i>	$C_D$	<i>Drag coefficient</i>
$V$	<i>Air velocity</i>	$C_L$	<i>Lift coefficient</i>
$\alpha$	<i>Angle of attack</i>	MAC	<i>Medium aerodynamic chord</i>
$p$	<i>Relative static pressure</i>	SIMPLE	<i>Semi IMPLICIT Pressure Linked Equation</i>
$A$	<i>Reference area</i>	STL	<i>Stereo Lithography (CAD files)</i>

## 1. INTRODUCTION

The range of unmanned aerial aircraft (UAV) is developing continuously generating new constructive solutions from small size and mass to those, which are comparable to piloted aircraft. The main reason of UAV use is due to lower cost of design, realization and operation (on flight hour) in comparison with human piloted aircraft. According to references [1, 2, 3, 4] UAV development included the flying wing (tailless) operating lonely or in network, see Fig. 1, [13, 14].



(a)



(b)

**FIG. 1** Flying wing UAV, a.Hirus-TeamNet), b. FireFLY6 flying wing-tricopter

Constructive solutions of flying wing UAV are characterized by a series of requirements and exploitation limits on whole cycle of conception, fabrication and testing. UAV requirements and exploitation limits can be grouped on the following

categories: design concepts, aero-mechanical, materials and technologies, testing methods, flight safety and security and economical [5, 6, 7, 15 and 16].

**2. CFD STUDIES FOR FLYING WING UAV**

**2.1. Preprocessing of model**

The mock-up geometry was rebuilt with Ansys DesignModeler and Catia starting from scanned digital model (STL format) see Fig. 2, [8].

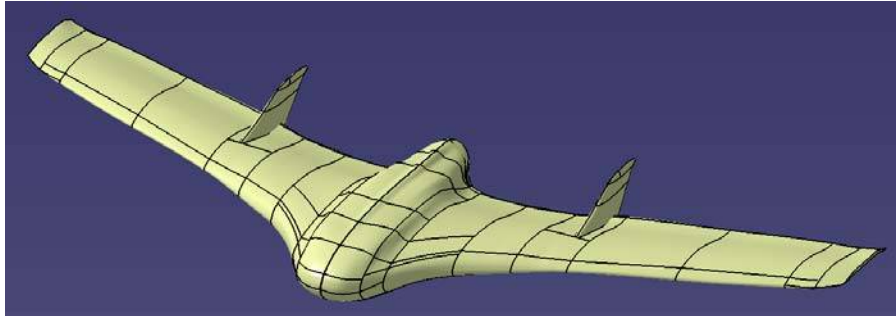


**FIG. 2** CFD model of flying wing

The mesh was generated with Numeca/Hexpress and has 3.8 millions of hexahedral cells. The grid is refined to properly capture the leading and trailing edge curvature the junction between wing and vertical empennage, see Figs. 3 and 4, [11, 12].

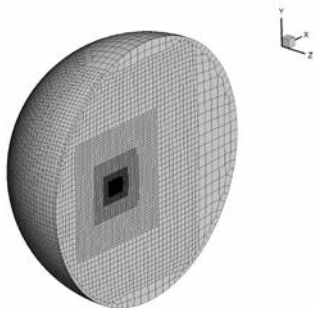


**FIG. 3** Computational domain and mesh



**FIG. 4** Mesh on flying wing surface

**2.2. Computational Cases**

The solver used in this study was Ansys Fluent [8]. In order to reduce the computational effort, a symmetry plane was introduced.

The governing equations are the Euler system. Furthermore, the fluid is assumed incompressible because the infinite upstream velocity is low (30 m/s). To solve numerically the Euler system, we used the SIMPLE algorithm due to its robustness and convergence rate for incompressible flows [9, 10]. The computational cases are given in table 1.

Table 1. Computational cases

Velocity (V)	30 m/s									
Angle of attack $\alpha(^{\circ})$	-6	-4	-2	0	3	3	9	12	15	18

The reference values used to obtain lift and drag coefficients and relative pressure are given in Table 2.

Table 2. Reference parameters

p	101325 Pa	$\rho$	1,225 kg/m <sup>3</sup>
A	0.29 m <sup>2</sup>	V	30 m/s

**2.3. Results and discussions**

The CFD results are given in table 3 and in Figs. 6-9.

Table 3 CFD results

V	30 m/s									
$\alpha$	-6 <sup>0</sup>	-4 <sup>0</sup>	-2 <sup>0</sup>	0 <sup>0</sup>	3 <sup>0</sup>	6 <sup>0</sup>	9 <sup>0</sup>	12 <sup>0</sup>	15 <sup>0</sup>	18
C <sub>L</sub>	0,074	0,227	0,383	0,538	0,760	0,944	1,012	1,007	0,926	0,901
C <sub>D</sub>	0,005	0,007	0,0013	0,023	0,043	0,070	0,154	0,234	0,286	0,325
C <sub>L</sub> /C <sub>D</sub>	15,113	31,400	29,133	23,763	17,660	13,514	6,581	4,294	3,238	2,771

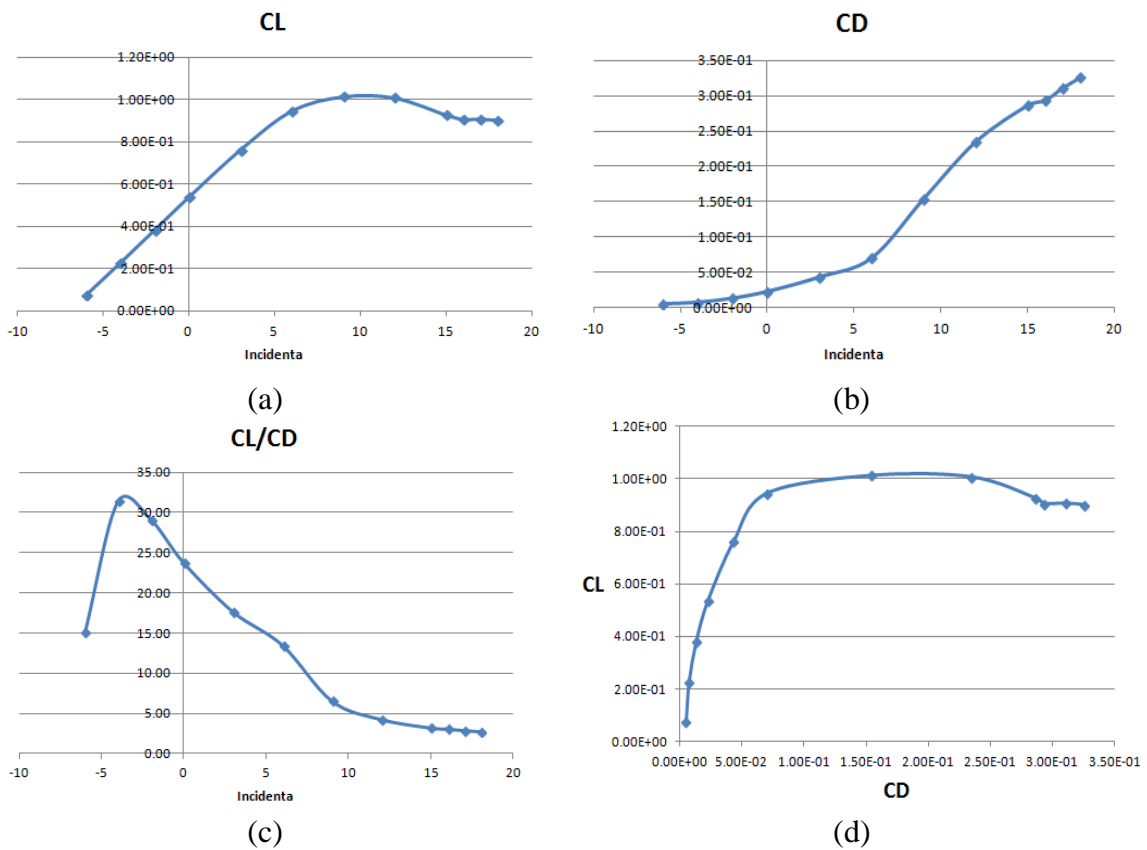


**FIG. 5** Computed aerodynamic parameters, a- lift coefficient, b-drag coefficient, c, d-lift to drag ratio (C<sub>L</sub>/C<sub>D</sub>)

According to table 3 and Fig. 5, the maximal value of lift coefficient is at angle of attack of 9<sup>0</sup>; significant increase of drag coefficient is observed from angles of attack greater than 6<sup>0</sup>.

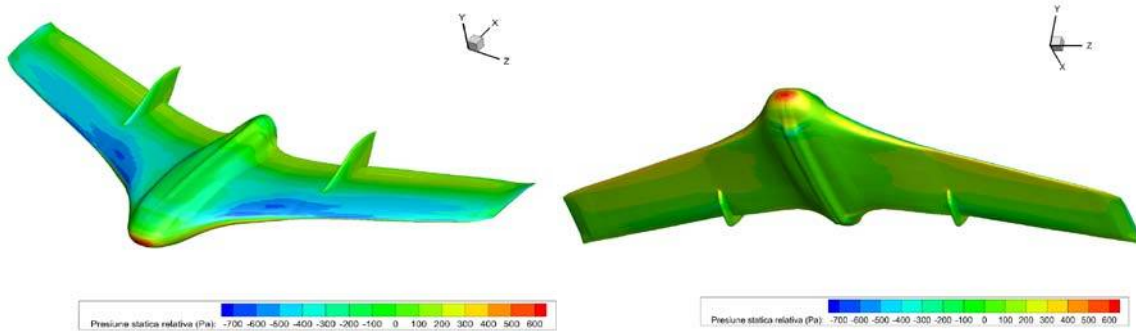


**FIG. 6** Relative static pressure (Pa) at angle of attack of  $0^{\circ}$  (suction side-pressure side)

The position of model in the scanned geometry was considered at angle of attack of  $0^{\circ}$ . One observes an incidence phase difference from the visualization of CAD model and from the comparison between CFD and wind tunnel results, see Fig. 6.

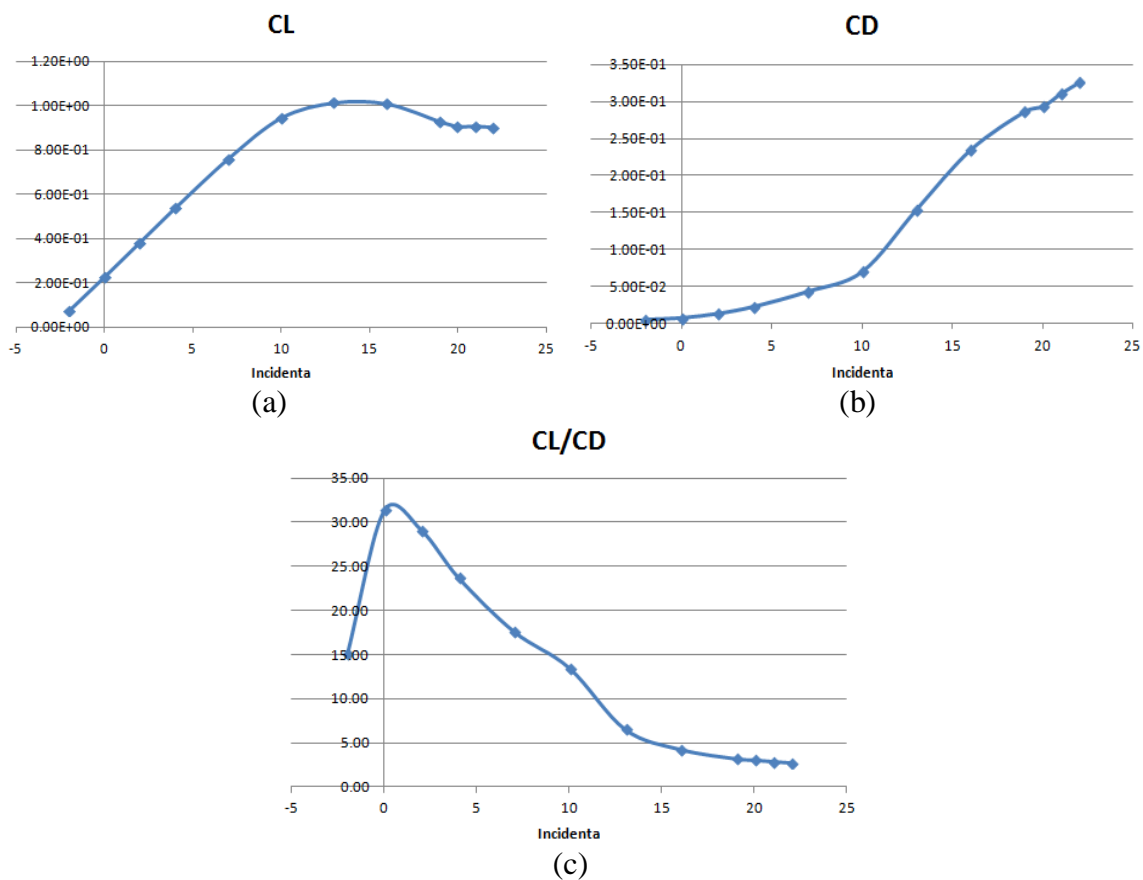


**FIG. 7** Aerodynamic parameters of a incidence phase difference of  $4^{\circ}$

One observes that the maximal lift coefficient is achieved for the angle of attack in the range  $12^{\circ}$  to  $13^{\circ}$ , see Fig. 7a; a significant increase of drag coefficient appears at angles of attack higher than  $10^{\circ}$  and the maximal lift to drag ratio is at angle of attack of around  $1^{\circ}$ , see Fig. 7c. The pressure difference on the pressure side and suction side of wing gives the lift. This is clearly illustrated in Fig. 8 and Fig 9.

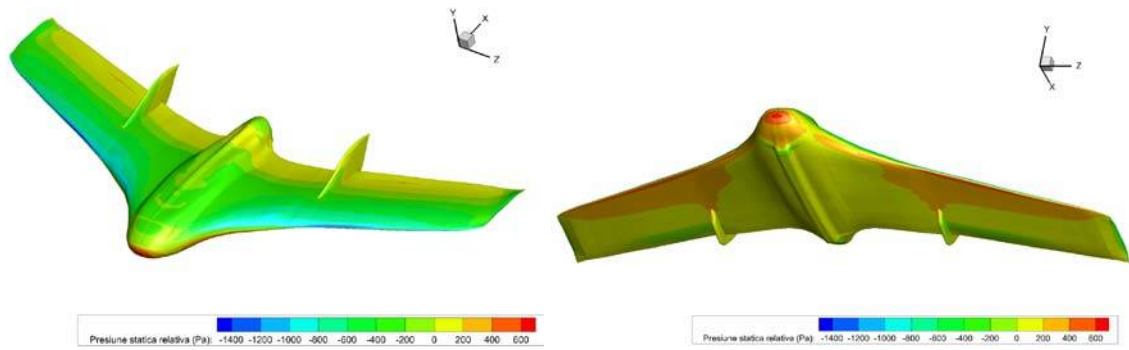


**FIG. 8** Relative static pressure distribution on the suction side (left side) and pressure side (right side) for angle of attack of  $3^{\circ}$

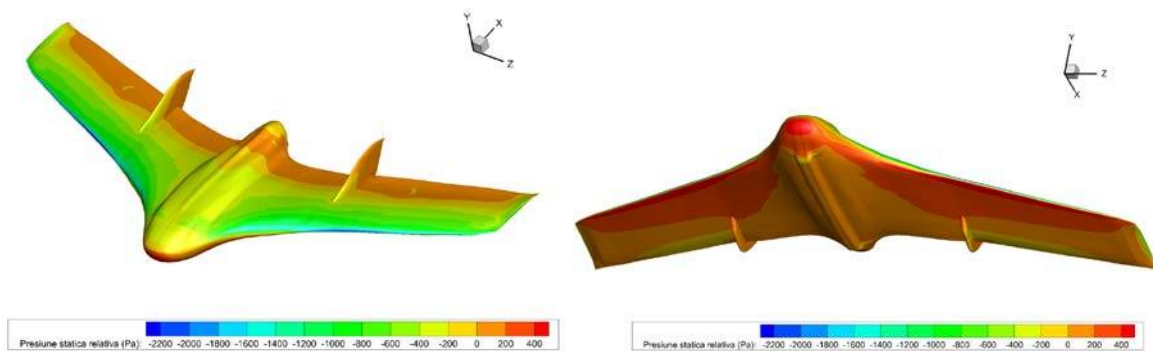


**FIG. 9** Relative static pressure distribution on the suction side (left side) and pressure side (right side) for angle of attack of  $6^{\circ}$

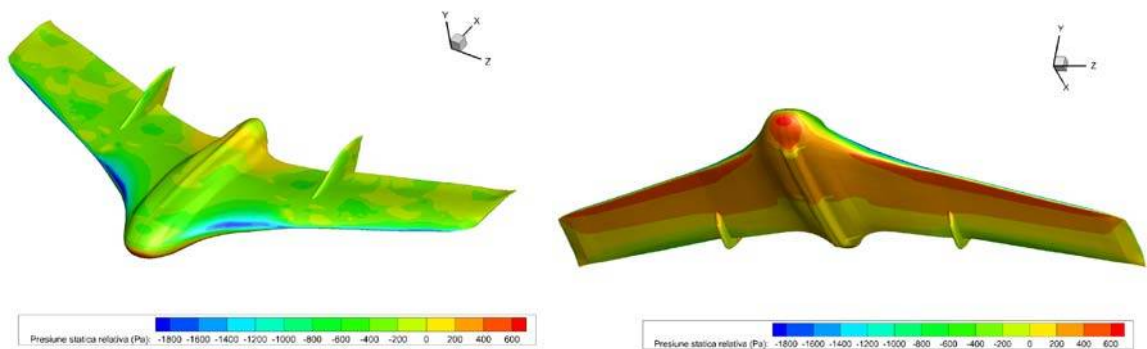


**FIG. 10** Relative static pressure distribution on the suction side (left side) and pressure side (right side) for angle of attack of  $12^{\circ}$

### 3. CONCLUSIONS AND NEW RESEARCH DIRECTIONS

This CFD analysis for a flying wing UAV shows that the aerodynamic optimization is necessary. Furthermore, the CFD results have to be validated with the experimental ones obtained in subsonic wind tunnel. The above analysis shows the aerodynamic characteristics for a flying wing UAV obtained through 3D scan and simplified geometry in junction zones (wing- vertical empennages).

For a better analysis, it is necessary a finer mesh, which is suitable for RANS computations. Moreover, it is necessary to increase the number of test cases for a velocity range from 0 to 35 m/s and an angle of attack range from  $-10^{\circ}$  to  $20^{\circ}$ . The future CFD

analyses could include the flights with the gliding angle up to 10° and with different twist angles.

### ACKNOWLEDGMENT

This work is supported by the Executive Agency for Higher Education, Research, Development and Innovation Funding (UEFISCDI) under MASIM project (PN-II-PT-PCCA-2013-4-1349).

### REFERENCES

- [1] *Unmanned Aircraft System ROADMAP 2005-2030*, US DoD, Washington DC, 2005, 213p.
- [2] UAS Yearbook, *Unmanned aircraft systems, The Global Perspective 2014/2015*, Blyenburg & Co, june 2014, Paris, ISSN 2270-6062, 240 p., available at [www.uvs-info.com](http://www.uvs-info.com).
- [3] Austin R., *Unmanned Aircraft Systems – UAVs design, development and deployment*, Aerospace series, Wiley and Sons Ltd publication, 2010, ISBN 978-0-470-05819-0, 365p.
- [4] Prisacariu V., Cîrciu I., Cioacă C., Boşcoianu M., Luchian A., *Multi aerial system stabilized in altitude for information management*, REVIEW OF THE AIR FORCE ACADEMY, 3(27)/2014, Braşov, Romania, ISSN 1842-9238; e-ISSN 2069-4733, p 89-94.
- [5] Prisacariu V., Boşcoianu M., Luchian A., *Innovative solutions and UAS limits*, REVIEW OF THE AIR FORCE ACADEMY, 2(26)/2014, Braşov, Romania, ISSN 1842-9238; e-ISSN 2069-4733, p51-58.
- [6] Reglementările aeronautice române RACR-AZAC, 2007, <http://www.caa.ro>, consulted at 03.04.2016
- [7] Directiva de navigabilitate privind aeronavele civile motorizate fără pilot uman la bord (UAV) DN 14-02-001, available at [http://www.caa.ro/pdf/Directiva%20identificare %20UAV.pdf](http://www.caa.ro/pdf/Directiva%20identificare%20UAV.pdf), consulted at 01.03.2014
- [8] ANSYS FLUENT User's Guide 14, 2011, 2948p
- [9] Patankar S. V., Spalding D., *A calculation procedure for heat, mass and momentum transfer in three dimensional parabolic flows*. 15:1787—1806, 1972
- [10] Dănăilă S. Berbente C., *Metode numerice in dinamica fluidelor*, Editura Academiei Române, Bucureşti, 2003.
- [11] Cojocaru, M. G., Niculescu, M. L., & Pricop, M. V. (2015). Aero-Acoustic assessment of installed propellers. *INCAS Bulletin*, ISSN 2066-8201, 7(2), p 53.
- [12] Tomac, M. and Eller, D., 2011. From geometry to CFD grids—an automated approach for conceptual design. *Progress in Aerospace Sciences*, 47(8), pp.589-596.
- [13] <http://www.aft.ro>, consulted at 01.04.2016
- [14] <http://www.birdseyeview.aero> consulted at 04.04.2016
- [15] Prisacariu V., Boscoianu M., Cîrciu I., *Morphing wing concept for small UAV*, APPLIED MECHANICS AND MATERIALS, Vol. 332 (2013) pp 44-49, ISSN: 1662-7482, © (2013) Trans Tech Publications, Switzerland, doi:10.4028/www.scientific.net /AMM.332.44 OPTIROB 2013.
- [16] Udriou R., Applications of additive manufacturing technologies for aerodynamic tests, ACADEMIC JOURNAL OF MANUFACTURING ENGINEERING, ISSN 1583-7904, VOL. 8, ISSUE 3/2010